Molecular and Electronic Structure of Octahedral *o*-Aminophenolato and *o*-Iminobenzosemiquinonato Complexes of V(V), Cr(III), Fe(III), and Co(III). Experimental Determination of Oxidation Levels of Ligands and Metal Ions

Hyungphil Chun, Claudio Nazari Verani, Phalguni Chaudhuri,* Eberhard Bothe, Eckhard Bill, Thomas Weyhermüller, and Karl Wieghardt*

Max-Planck-Institut für Strahlenchemie, Stiftstrasse 34−36, D-45470 Mülheim an der Ruhr, Germany

Received January 25, 2001

The coordination chemistry of the ligands 2-anilino-4,6-di-*tert*-butylphenol, H[L^{AP}], and *N*,*N*‴-bis{2-(4,6-di-*tert*-butylphenol}diethylenetriamine, $H_2[(L^{AP})N(L^{AP})]$, has been studied with the first-row transition metal ions V, Cr, Fe, and Co. The ligands are noninnocent in the sense that the aminophenolato parts, $[L^{AP}]^-$ and $[L^{AP}-H]^{2-}$, can be readily oxidized to their *o*-iminobenzosemiquinonato, $[L^{ISQ}]^-$, and *o*-iminobenzoquinone, [L^{ISB}], forms. The following neutral octahedral complexes have been isolated as crystalline materials, and their crystal structures have been determined by X-ray crystallography at 100 K: $[Cr^{III}(L^{ISQ})_3]$ (**1**), $[Fe^{III}(L^{ISQ})_3]$ (**2**), $[Co^{III}(L^{ISQ})_3]$ (**3**), $[V^V(L^{ISQ})(L^{AP}-H)_2]$ (**4**), $[V^V(L^{AP}-H)_2(L^{AP})]$ (**5**), and $[V^VO\{(L^{AP})N(L^{AP}-H)\}]$ (**6**). From variable-temperature magnetic susceptibility measurements and X-band EPR spectroscopy it has been established that they possess the ground states: **1**, $S = 0$; **2**, $S = 1$; **3**, $S = {}^3/_2$; **4**, $S = {}^1/_2$; **5**, $S = 0$; **6**, $S = 0$. The *o*-iminobenzosemiquinonato radicals ($S_{rad} = {}^1/_2$) couple strongly intramolecularly antiferromagnetically to singly occupied orbitals of the t_{2g} subshell at the respective metal ion but ferromagnetically to each other in **3** containing a Co^{III} ion with a filled t_{2g}^6 subshell. It is demonstrated that the oxidation level of the ligands and metal ions can be unequivocally determined by high-quality X-ray crystallography in conjunction with EPR, UV−vis, and Mössbauer spectroscopies. The spectro- and electrochemistry of these complexes have also been studied in detail. Metal- and ligand-based redox chemistry has been observed. The molecular and electronic structures are compared with those of their *o*-semiquinonato analogues.

Introduction

o-Catecholates are probably the archetypal noninnocent ligands in coordination chemistry.[1,2] They exist in three distinctly different oxidation levels in complexes: they bind in an *O*,*O*-bidentate fashion, as catecholato dianions ($S = 0$), as *o*-semiquinonato monoanions ($S = {}^1/_2$), or as neutral *o*-benzoquinones ($S = 0$). It has been firmly established by X-ray crystallography that the geometries of these ligands differ in a systematic manner depending on the respective oxidation level. Three parameters serve as markers: (i) the average of the two C−O bond distances in the ortho-position shrinks from ∼1.35 Å in catecholates to ∼1.30 Å in semiquinonates to ∼1.24 Å in benzoquinones, (ii) concomitantly, the sum of the six C−C distances of the ring increases with increasing oxidation level and, in addition, (iii) these six C−C bond distances are nearly equivalent in catecholates, but display a pattern of short−long−short C−C distances in semiquinonates (quinoid structure) and more pronounced so in quinones. Similar observations have been reported for *o*-phenylenediamides and their two oxidized forms, namely, the *o*-diiminobenzosemiquinonates and *o*-diiminoquinones.[3]

We have recently begun to study the coordination chemistry of *o*-aminophenols which may be viewed as a hybrid of the two above ligand systems.[4] The ligand 2-anilino-4,6-di-*tert*-butylphenol (Scheme 1) has been shown to be noninnocent; it can bind as *o*-aminophenolate, $(L^{AP})^-$, or in its O- and N-deprotonated amidophenolate form, $(L^{AP}-H)^{2-}$, but it can also be oxidized and bind as *o*-iminosemiquinonate monoanion, which is a radical $(L^{ISQ})^{\bullet -}$. From high-quality low-temperature X-ray structure determinations, it has been established that neutral square-planar complexes $[M(L^{ISQ})_2]$ ($M = Cu^{II}$, Ni^{II}, Pd^{II}, Pt^{II}) contain two *O*,*N*-coordinated *o*-iminosemiquinonato(1−) ligands. Thus the diamagnetic Ni^{II}, Pd^{II}, Pt^{II} complexes are diradicals with a singlet ground state.[4] In contrast, in octahedral $[Co^{III}(L^{ISQ})_3]$ the three radical ligands couple intramolecularly ferromagnetically yielding an $S = {}^3/_2$ ground state.[5] Importantly, the above geometric features i, ii, and iii for *o*-semiquinonato complexes are very similar for compounds containing the *o*-iminobenzosemiquinonato radical ligand.

Here we report the synthesis, the electronic and molecular structure of a series of octahedral complexes of V, Cr, Fe, and Co containing three O,N-coordinated ligands of the type $(L^{AP}-H)^{2-}$, $(L^{AP})^-$, or $(L^{ISQ})^{\bullet -}$. An important aspect of this work relates to the question of whether it is possible to discern from structural parameters between a coordinated monoanion $(L^{AP})^-$, a dianion $(L^{AP}-H)^{2-}$, and its one-electron oxidized form $(L^{ISQ})^{\bullet -}$ or not. We will show that high-quality X-ray crystallography in conjunction with spectroscopy allows in all cases investigated an unambiguous assignment of the oxidation level (state) of the ligands and metal ion in a given compound.

(1) Pierpont, C. G.; Buchanan, R. M. *Coord. Chem. Rev.* **1981**, *38*, 45.
(2) Pierpont, C. G.; Lange, C. W. *Progr. Inorg. Chem.* **1994**, *41*, 331.
(3) Mederos, A.; Dominguez, S.; Hernández-Molina, R.; Sanchiz, J.; Brito, F. *Coord. Chem. Rev.* **1999**, *193−195*, 913.
(4) Chaudhuri, P.; Verani, C. N.; Bill, E.; Bothe, E.; Weyhermüller, T.; Wieghardt, K. *J. Am. Chem. Soc.* **2001**, *123*, 2213.
(5) Verani, C. N.; Gallert, S.; Bill, E.; Weyhermüller, T.; Wieghardt, K.; Chaudhuri, P. *Chem. Commun.* **1999**, 1747.

10.1021/ic010106a CCC: $20.00
Published on Web 07/07/2001

Scheme 1. Ligands and Complexes

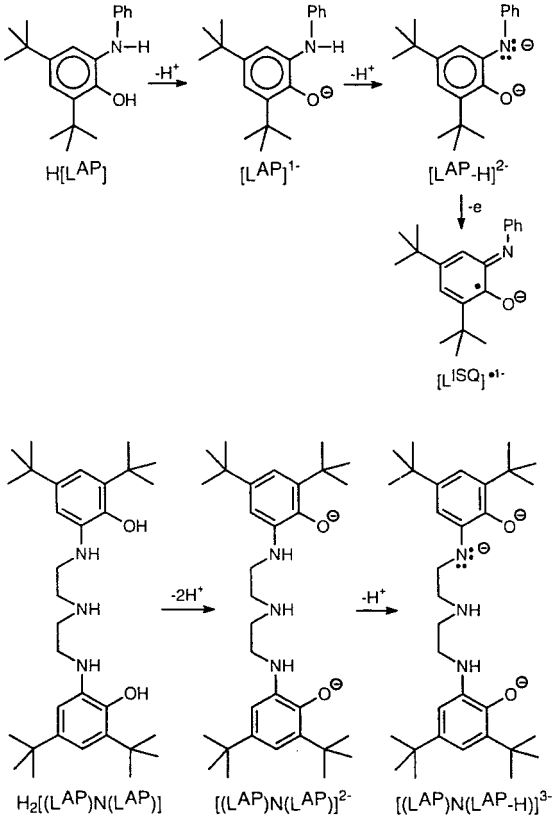

Complexes: $[Cr^{III}(L^{ISQ})_3]$ **1**

$[Fe^{III}(L^{ISQ})_3]$ **2**·

$[Co^{III}(L^{ISQ})_3]$ **3**

$[V^{V}(L^{ISQ})(L^{AP}\text{-}H)_2]$ **4**

$[V^{V}(L^{AP}\text{-}H)_2(L^{AP})]$ **5**

$[V^{V}O\{(L^{AP})N(L^{AP}\text{-}H)\}]$ **6**

We also describe the synthesis of a new pentadentate ligand *N*,*N*‴-bis{2-(4,6-di-*tert*-butylphenol}diethylenetriamine, $H_2[(L^{AP})N(L^{AP})]$, shown in Scheme 1, and its complex $[V^{V}O\{(L^{AP})N(L^{AP}-H)\}]$.

Experimental Section

The ligand 2-anilino-4,6-di-*tert*-butylphenol, $H[L^{AP}]$, has been prepared according to published procedures.[4,6]

Preparation of *N*,*N*‴-Bis{2-(4,6-di-tert-butylphenol)}diethylenetriamine, $H_2[(L^{AP})N(L^{AP})]$. To a solution of 3,5-di-*tert*-butylcatechol (2.25 g; 10.1 mmol) in warm *n*-heptane (30 mL) was added diethylenetriamine (0.76 mL; 7.0 mmol) and triethylamine (1.0 mL). After being heated to reflux for 30 min, the solution was cooled to 20 °C and stored at 0 °C overnight. A colorless precipitate was isolated by filtration and washed with small amounts of cold *n*-heptane:. yield, 2.2 g (86%); mp (uncorrected), 157−159 °C. ^{1}H NMR (250 MHz, $CDCl_3$, 300 K): δ 1.25 (s, 18H), 1.39 (s, 18H), 2.69 (s, 2H), 2.84 (s, 2H), 3.77 (s, 4H), 6.68−6.81 (m, 4H). ^{13}C {H}NMR (100.6 MHz, $CDCl_3$, 300 K): δ 29.84, 31.64, 34.27, 34.86, 40.98, 51.30, 110.61, 115.13, 135.46, 141.61, 141.67, 143.41. Anal. Calcd for $C_{32}H_{53}N_3O_3$: C, 75.10; H, 10.34; N, 8.21. Found: C, 75.3; H, 10.1; N, 8.0.

$[Cr^{III}(L^{ISQ})_3]$ (1). To a solution of $[Cr^{III}(THF)_3Cl_3]$ (0.38 g; 1.0 mmol) (THF = tetrahydrofuran) and triethylamine (0.9 mL) in acetonitrile (30 mL) was added the ligand $H[L^{AP}]$ (0.90 g; 3 mmol). The mixture was heated to reflux with stirring for 2 h in the presence of air and then cooled to 20 °C. After adding an additional amount of NEt_3 (0.45 mL), the dark reddish solution was allowed to stand in an open vessel in air. A dark red-black powder formed which was collected after 5 days: yield, 0.49 g (52%). Recrystallization of this material from a saturated acetone solution at ambient temperature afforded black single-crystals suitable for X-ray diffraction. ^{1}H NMR (250 MHz, acetone-d_6, 300 K): δ 1.03 (s, 9H), 1.11 (s, 9H), 1.25 (s, 9H), 1.32 (s,sh, 18H), 1.48 (s, 9H); 3.52 (d, 1H), 3.61 (s,br, 1H), 5.20−5.43 (m, 9H), 6.65 (m, 5H), 7.38 (s,br, 2H), 7.80 (s,br, 2H), 8.27 (s,br, 1H). EI mass spectrum: m/z = 938 $\{M\}^+$, 642 $\{M - L\}^+$. Anal. Calcd for $C_{60}H_{75}N_3O_3Cr$: C, 76.72; H, 8.06; N, 4.47, Cr, 5.54. Found: C, 76.7; H, 7.9; N, 4.4; Cr, 5.6.

$[Fe^{III}(L^{ISQ})_3]$ (2). To a solution of $H[L^{AP}]$ (1.58 g; 5.3 mmol) in methanol (40 mL) was added $FeCl_2 \cdot 4H_2O$ (0.18 g; 0.9 mmol) and NEt_3 (0.8 mL). This mixture was heated to reflux in the presence of air for 1 h. From the filtered solution a dark green, crystalline precipitate formed upon slow cooling to room temperature. Yield: 0.49 g (57%). A single-crystal suitable for X-ray diffraction was selected from the crude product. EI mass spectrum: m/z = 941 $\{M\}^+$, 646 $\{M - L\}^+$, 297 $\{M - 2L - Fe\}^+$. Anal. Calcd for $C_{60}H_{75}N_3O_3Fe$: C, 76.49; H, 8.02; N, 4.46. Found: C, 76.3; H, 8.1; N, 4.4.

$[Co^{III}(L^{ISQ})_3]$ (3). This complex was prepared as described in refs 4 and 5.

$[V^{V}(L^{AP}-H)_2(L^{ISQ})]$ (4). To a solution of $H[L^{AP}]$ (0.90 g; 3 mmol) in CH_3CN (30 mL) was added $V(THF)_3Cl_3$ (0.37 g; 1.0 mmol), NEt_3 (0.70 mL), and triphenylphosphine (0.26 g; 1.0 mmol). The mixture was heated to reflux in the presence of air for 1 h. The dark blue solution was allowed to stand in an open vessel for 24 h after addition of 0.5 mL of NEt_3. A dark blue-black microcrystalline precipitate formed which was collected by filtration: yield, 0.51 g (55%). Single-crystals suitable for X-ray crystallography were obtained from a saturated acetone solution by slow evaporation of the solvent. EI mass spectrum: m/z = 936 $\{M\}^+$, 641 $\{M - L\}^+$, 468 $\{M\}^{2+}$. Anal. Calcd for $C_{60}H_{75}N_3O_3V$: C, 76.89; H, 8.07; N, 4.48. Found: C, 76.8; H, 8.1; N, 4.4.

$[V^{V}(L^{AP}-H)_2(L^{AP})]$ (5). To a solution of the ligand $H[L^{AP}]$ (0.89 g; 3.0 mmol) in acetonitrile (30 mL) under an argon atmosphere was added $VO(SO_4) \cdot 5H_2O$ (0.25 g; 1.0 mmol) in small amounts. Upon addition of NEt_3 (1.0 mL) the color of the solution turned to dark green. After being heated to reflux for 1 h, the then dark blue solution was allowed to stand at ambient temperature in the presence of air. Small crystals precipitated which were collected by filtration: yield, 0.26 g (26%). ^{1}H NMR (500 MHz, $CDCl_3$, 300 K): δ 0.89 (s, 9H), 0.97 (s, 9H), 1.11 (s, 9H), 1.17 (s, 9H), 1.28 (s, 9H), 1.32 (s, 9H), 6.3−7.1 (m, 21H). EI mass spectrum: m/z = 937 $\{M\}^+$, 641 $\{M - L\}^+$, 626 $\{M - L - CH_3\}^+$, 295 $\{M - 2L - V\}^+$. Anal. Calcd for $C_{60}H_{76}N_3O_3V$: C, 76.81; H, 8.17; N, 4.48; V, 5.43. Found: C, 76.7; H, 7.9; N, 4.4; V, 5.4.

$[V^{V}O\{(L^{AP})N(L^{AP}-H)\}]$ (6). Under an argon blanketing atmosphere the ligand $H_2[(L^{AP})N(L^{AP})]$ (0.51 g; 1.0 mmol) was dissolved in acetonitrile (30 mL) at 40 °C. To this clear solution was added a solid sample of $[N(Et)_4][VOBr_4]$ (0.52 g; 1.0 mmol) in small amounts. Upon addition of NEt_3 (1.0 mL) the color of the solution changed to dark violet. After being heated to reflux for 1 h, the solution was cooled to ambient temperature and filtered. From this solution violet crystals of X-ray quality precipitated, which were collected by filtration: yield, 0.27 g (47%). IR (KBr disk): 3155 ν(N−H), 916 ν(V=O). ^{1}H NMR (500 MHz, $CDCl_3$, 300 K): δ 0.97 (s, 9H), 1.17 (s, 9H), 1.32 (s, 9H), 1.50 (s, 9H), 2.22 (m, 1H), 2.41 (m, 1H), 2.78 (m, 1H), 2.87 (m, 1H), 3.00 (m, 1H), 3.40 (m, 1H), 4.48 (m, 1H), 4.80 (m, 1H), 5.02 (m, 1H), 6.00 (b, 1H), 6.26 (d, 1H), 6.68 (d, 1H), 6.76 (d, 1H), 7.05 (d, 1H). (131.55 MHz, $CDCl_3$, 300 K): δ 235.26. ^{51}V NMR (CD_3CN, 300 K): δ 195.19. ($VOCl_3$ standard).ESI mass spectrum (pos. ion): m/z = 576 $\{M + H\}^+$. Anal. Calcd for $C_{32}H_{50}N_3O_3V$: C, 66.76; H, 8.75; N, 7.30; V, 8.85. Found: C, 66.8; H, 8.6; N, 7.3; V, 8.8.

Physical Measurements. Electronic spectra of the complexes and spectra of the spectroelectrochemical investigations were recorded on

(6) (a) Maslovskaya, L. A.; Petrikevich, D. K.; Timoshchuk, V. A.; Shadyro, O. I. *Russ. J. Gen. Chem.* **1996**, *66*, 1842. Translated from: *Zh. Obsh. Khim.* **1996**, *66*, 1893. (b) FRG Patent no. 1104522; 1959; *Chem. Abstr*. **1962**, *56*, 5887.

Table 1. Crystallographic Data

	1	**2**	**4**	**5**	**6**
empirical formula	$C_{60}H_{75}CrN_3O_3$	$C_{60}H_{75}FeN_3O_3$	$C_{60}H_{75}N_3O_3V$	$C_{60}H_{76}N_3O_3V$	$C_{32}H_{50}N_3O_3V$
FW	938.23	942.08	937.17	938.18	575.69
space group	$P2_12_12_1$, No. 19	$P2_12_12_1$, No. 19	$P2_12_12_1$, No. 19	$P\bar{1}$, No. 2	$C2/c$, No. 15
a, Å	12.9544(8)	12.9898(14)	12.9697(9)	15.165(2)	34.225(5)
b, Å	17.7004(12)	17.483(2)	17.748(2)	18.128(2)	6.7592(8)
c, Å	23.295(2)	23.634(3)	23.101(2)	21.961(2)	28.552(3)
α, deg	90	90	90	93.41(2)	90
β, deg	90	90	90	97.10(2)	105.33(2)
γ, deg	90	90	90	112.67(2)	90
V, Å	5341.5(7)	5367.3(11)	5317.5(8)	5490.2(12)	6370.0(14)
Z	4	4	4	4	8
T, K	100(2)	100(2)	100(2)	100(2)	100(2)
ρ_{calcd}, g cm^{-3}	1.167	1.166	1.171	1.135	1.201
reflcns collected/$2\theta_{max}$	28 246/60.0	22 449/45.0	19 609/56.0	43 486/50.0	23 229/50.0
unique reflns/$I > 2\sigma(I)$	15 071/12787	7004/4709	12 058/9674	18 784/11630	5539/3880
no. of params/restr	622/0	604/3	624/132	1283/6	352/0
μ(Mo Kα), cm^{-1}	2.60	3.27	2.33	2.25	3.46
R1[a]	0.0472	0.0518	0.0699	0.0517	0.0714
wR2[b] ($I > 2\sigma(I)$)	0.1035	0.0844	0.1467	0.1180	0.1678

[a] Observation criterion: $I > 2\sigma(I)$. $R1 = \Sigma||F_o| - |F_c||/\Sigma|F_o|$. [b] $wR2 = [\Sigma[w(F_o^2 - F_c^2)^2]/\Sigma[w(F_o^2)^2]]^{1/2}$, where $w = 1/\sigma^2(F_o^2) + (aP)^2 + bP$, $P = (F_o^2 + 2F_c^2)/3$.

a HP 8452 A diode array spectrophotometer (range: 220−1100 nm). Cyclic and square-wave voltammograms and Coulometric experiments were performed using an EG&G potentiostat/galvanostat. Variable-temperature (2−298 K) magnetization data were recorded on a SQUID magnetometer (MPMS Quantum design) in an external magnetic field of 1.0 T. The experimental susceptibility data were corrected for underlying diamagnetism by the use of tabulated Pascal's constants. X-band EPR spectra were recorded on a Bruker ESP 300 spectrometer. The spectra were simulated by iteration of the (an)isotropic g values, hyperfine coupling constants, and line widths. We thank Dr. F. Neese (Abteilung Biologie der Universität Konstanz) for a copy of his EPR simulation program. NMR experiments were carried out on Bruker ARX 250, 500 spectrometers (250, 500, and 63 MHz for ^{1}H and ^{13}C NMR, respectively). The internal shift reference for ^{1}H NMR, with CHD_2CN, is $\delta_H = 1.94$; the internal shift reference for ^{13}C NMR, with CD_3CN, is $\delta_C = 118.3$. The ^{57}Fe Mössbauer spectrum was measured on an Oxford Instruments Mössbauer spectrometer in zero-field. ^{57}Co/Rh was used as radiation source. The temperature of the sample was controlled by an Oxford Instruments Variox Cryostat. Isomer shifts were determined relative to α-iron at 300 K. The minimum experimental line width was 0.24 mm s^{-1}.

X-ray Crystallographic Data Collection and Refinement of the Structures. Dark red single crystals of **1** and **5**, a black crystal of **2**, a deep blue crystal of **4**, and a dark violet specimen of **6** were fixed with perfluoropolyether on glass fibers. Crystals of **1**, **2**, and **4** were mounted on a Nonius Kappa-CCD diffractometer; **5** and **6** were measured on a Siemens SMART system. Both diffractometers were equipped with a cryogenic nitrogen cold stream operating at 100(2) K. Graphite monochromated Mo−Kα radiation (λ = 0.710 73 Å) was used. Crystallographic data of the compounds are listed in Table 1. Final cell constants were obtained from a least-squares fit of the setting angles of several thousand strong reflections. Intensity data were corrected for Lorentz and polarization effects. Intensity data of **1** and **4** were corrected for absorption using the program MulScanAbs embedded in the PLATON99 program suite.[7a] The program SADABS[7b] was used for absorption correction of **5**. The crystal faces of **6** were determined and a Gaussian type correction via XPREP[8] was used here, while the data set of **2** was left uncorrected. The Siemens ShelXTL[8] software package was used for solution, refinement, and artwork of the structures and neutral atom scattering factors of the program were used. All structures were solved and refined by direct methods and difference Fourier techniques. Non-hydrogen atoms were refined anisotropically. Hydrogen atoms were placed at calculated positions and refined as riding atoms with isotropic displacement parameters. Split atom models were used to account for disorder of *tert*-butyl groups in complexes **4** and **5**. The two positions were refined with restrained C−C distances being equal within errors using the SADI instruction in SHELXL.

(7) (a) Spek, A. L. University of Utrecht, The Netherlands, 1999. (b) SADABS, Sheldrick, G. M. Universität Göttingen, 1994.
(8) *ShelXTL*, Version 5; Siemens Industrial Automation; Inc.: 1994.

Results

Syntheses and Characterization of Complexes. Preparations of mononuclear complexes containing three O,N-coordinated, bidentate ligands derived from H[L^{AP}] have been performed in a straightforward fashion in methanol or acetonitrile solutions.

The reaction of a suitable starting material like [$Cr^{III}(THF)_3Cl_3$], $Fe^{II}Cl_2\cdot 4H_2O$, [$V(THF)_3Cl_3$], $VO(SO_4)\cdot 5H_2O$, or [NEt_4][$VOBr_4$] with 3 equiv of H[L^{AP}] and a suitable base like NEt_3 and PPh_3 in the presence of air at elevated temperatures afforded in all cases highly colored microcrystalline materials which were recrystallized and analyzed by elemental analysis, EI and ESI (pos. ion) mass spectrometry. The following complexes have been obtained (Scheme 1): [$M^{III}(L^{ISQ})_3$] (M = Cr (**1**), Fe (**2**), Co (**3**)[4,5]), [$V^V(L^{AP}-H)_2(L^{ISQ})$] (**4**), and [$V^V(L^{AP}-H)_2(L^{AP})$] (**5**).

The reaction of 2 equiv of 3,5-di-*tert*-butylcatechol with 1 equiv diethylenetriamine in *n*-heptane in the presence of air yielded *N*,*N*‴-bis{2-{4,6-di-*tert*-butylphenol}diethylenetriamine, H_2[(L^{AP})N(L^{AP})] in 86% yield. This ligand reacted under an argon atmosphere with [NEt_4][$VOBr_4$] (1:1) in CH_3CN in the presence of NEt_3 to afford purple crystals of [V^VO{(L^{AP})-N($L^{AP}-H$)}] (**6**).

From variable-temperature (2−300 K) magnetic susceptibility measurements it was established that complexes **1**, **5**, and **6** are diamagnetic ($S = 0$ ground state). It is noted that all of these species possess significant temperature-independent paramagnetism. We have recorded the ^{1}H NMR spectra of these compounds (see Experimental Section). In agreement with the X-ray structure determinations complexes **1** and **5** display each six proton signals for six nonequivalent *tert*-butyl groups in the range $\delta = 0.89-1.48$, indicating C_1 symmetry for both pseudo-octahedral molecules. Similarly, for **6** we observed four such signals, indicating that the two aminophenol parts of the coordinated ligand are not equivalent.

Figure 1 displays the temperature dependence of the effective magnetic moments, μ_{eff}, of **1**, **2**, and **4**. Complex **2** possesses an $S = 1$ ground state, whereas for **4** it is $S = {}^1/_2$. In the temperature range 30−120 K these compounds display nearly

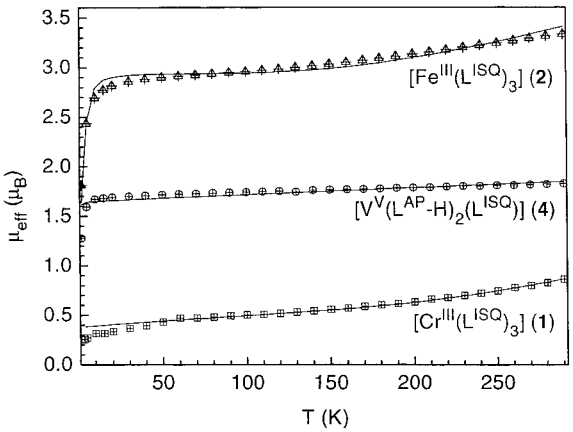

Figure 1. Temperature dependence of the magnetic moments, μ_B, of complexes **1**, **2**, and **4**. The solid lines represent fits; for parameters see text.

temperature-independent spin-only values typical for their respective ground state: for **2** it is 2.85−2.90 μ_B, and for **4** it is 1.70−1.75 μ_B. Above ∼120 K the magnetic moments of **1**, **2**, and **4** increase monotonically: At 300 K the magnetic moment for **4** is about 4% larger than that at 120 K, but for **2** it is 14%. Strong intramolecular antiferromagnetic coupling between a high-spin ferric ion (d^5) in **2**, and a Cr^{III} ion (d^3) in **1** with three organic radical ligands $(L^{ISQ})^{\bullet-}$ prevails yielding the observed ground states of $S = 0$ (**1**) and 1 (**2**). It is possible to fit this temperature dependence by using antiferromagnetic coupling constants for the coupling between the paramagnetic metal ion and three semiquinonate ligand radicals. The fits in Figure 1 were obtained by using the following parameters: $J_{12} = J_{13} = J_{14} = -436$ cm^{-1}, $g = 2.0$ (fixed), TIP $= 0.13 \times 10^{-3}$ cm^3 mol^{-1}, paramagnetic impurity 1% ($S = {}^3/_2$) for **1**; and $J_{12} = J_{13} = J_{14} = -120$ cm^{-1}, $g = 2.04$ for **2**. The convention $H = -2J\mathbf{S}_1 \times \mathbf{S}_2$ is used here.

In contrast, for **3** containing a low-spin cobalt(III) ion with a filled t_{2g}^6 subshell, we have previously shown that intramolecular *ferromagnetic* coupling yields an $S = {}^3/_2$ ground state (μ_{eff}(15K) $= 3.7\ \mu_B$).[5]

The iron containing species **2** contains a high-spin ferric ion (d^5) as was clearly established by its zero-field Mössbauer spectrum recorded at 80 K, which is shown in Figure S1 of the Supporting Information. An isomer shift, δ, of 0.54 mm s^{-1} and a quadrupole splitting parameter, $|\Delta E_Q|$, of 1.035 mm s^{-1} are diagnostic for octahedral high-spin ferric species.[9]

The X-band EPR spectrum of **4** in frozen CH_2Cl_2 solution at 60 K shown in Figure 2 (top) displays a nearly isotropic signal at $g = 2.0045$ confirming the $S = {}^1/_2$ ground state of **4**. No resolved ^{51}V hyperfine splitting has been observed, but from the width of the signal $A(^{51}V)$ cannot be larger than ∼5 G. These parameters rule out the description of **4** as a V(IV) (d^1) species with three diamagnetic ligands. Rather, it is characteristic of a coordinated ligand radical, $S_{rad} = {}^1/_2$, weakly coupled to the ^{51}V nuclear spin of $^7/_2$. This would be compatible with charge distributions $[V^{III}(L^{ISQ})_3]$, where two radical spins couple antiferromagnetically to a t_{2g}^2 configurated V(III) center, or $[V^{IV}(L^{ISQ})_2(L^{AP}-H)]$, or $[V^V(L^{ISQ})(L^{AP}-H)_2]$. As we show below, the structural data are indicative of the last formulation, with a ligand-centered radical and a diamagnetic V^V ion.

Crystal Structure Determinations. The crystal structures of complexes **1**, **2**, and **4**−**6** have been determined by single-crystal X-ray crystallography at 100 K. Figures 3−5 show the structures of the neutral molecules in crystals of **2**, **5**, and **6**, respectively. The structure of **3** has been communicated previously.[5] Figures S2 and S3 of the Supporting Information display the structures of the molecules in crystals of **1** and **4**, respectively; these structures are very similar to that of **2**. Selected metal-to-oxygen and metal-to-nitrogen bond lengths are summarized in Table 2; Table S26 of the Supporting Information gives a compilation of C−O, C−N, and C−C distances of each of the coordinated aminophenol parts in complexes **1**−**6**. All other bond distances and angles are available in the Supporting Information.

We describe the structure of **6** (Figure 5) first, because it allows the unambiguous assignment of the physical oxidation level for the ligand and the central vanadium ion. The geometric

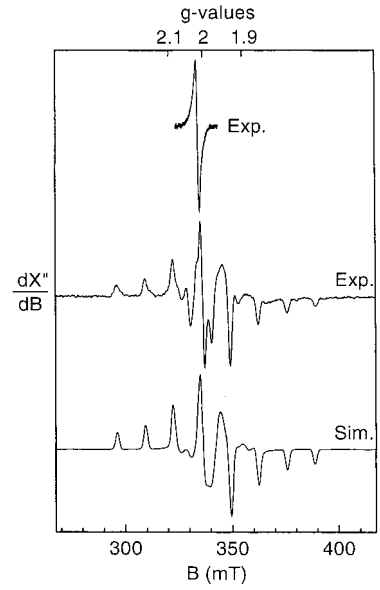

Figure 2. X-band EPR spectra recorded at 60 K in frozen CH_2Cl_2 solutions (0.10 M $[TBA]PF_6$) of **4** (top), its electrochemically 2e reduced form (middle), and its simulation (bottom). Experimental conditions: frequency, 9.4358 and 9.4371; microwave power, 0.2 and 0.1 mW; modulation amplitude, 0.99 and 1.25 mT for **4** and its dianion, respectively. Simulation parameters: $g_x = 1.963$, $g_y = 1.967$, $g_z = 1.984$; $W_x = 19.1$, $W_y = 10.3$, $W_z = 29.3$ G; $A_x = 50.8$, $A_y = 129.7$, $A_z = 7.2$ G (^{51}V; $I = {}^7/_2$, 100%).

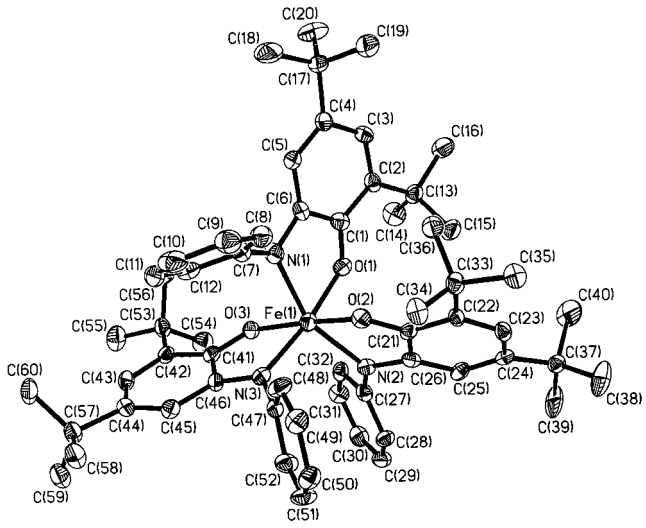

Figure 3. Structure of the neutral molecule in crystals of **2**.

(9) Snodin, M. D.; Ould-Moussa, L.; Wallmann, U.; Lecomte, S.; Bachler, V.; Bill, E.; Hummel, H.; Weyhermüller, T.; Hildebrandt, P.; Wieghardt, K. *Chem. Eur. J.* **1999**, *5*, 2554.

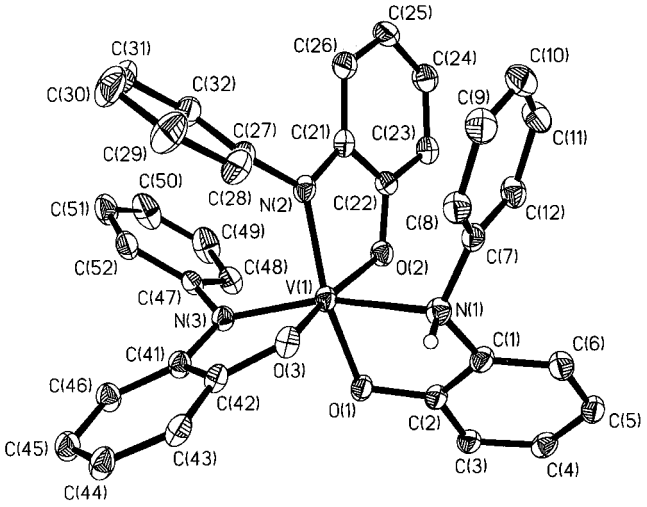

Figure 4. Structure of the neutral molecule in crystals of **5**. The six *tert*-butyl groups have been deleted for the sake of clarity: the open circle at N1 represents a hydrogen atom.

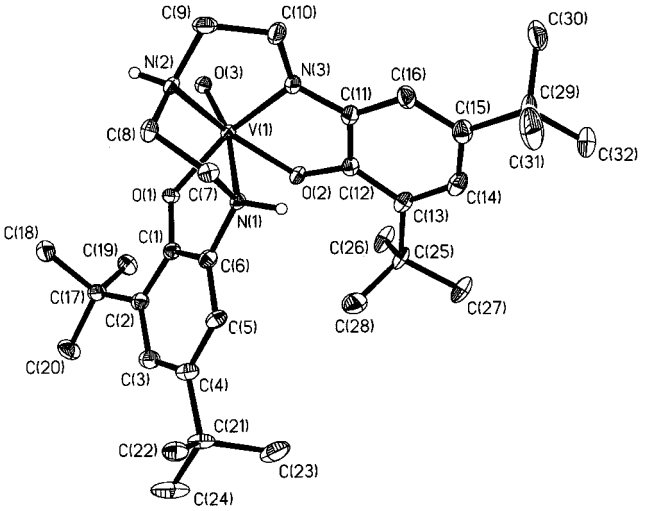

Figure 5. Structure of the neutral molecule in crystals of **6**. The open circles at N1 and N2 represent hydrogen atoms.

Table 2. Summary of M−O and M−N Bond Distances in Complexes **1**−**6**

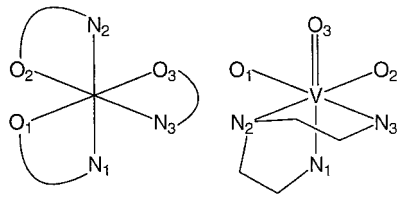

complex	M−O_1	M−O_2	M−O_3	M−N_1	M−N_2	M−N_3
1	1.943(1)	1.961(1)	1.958(1)	2.013(2)	2.030(2)	1.959(2)
2	2.015(3)	2.018(3)	2.009(3)	2.057(4)	2.149(4)	2.091(4)
3[a]	1.878(1)	1.896(1)	1.889(1)	1.937(1)	1.946(1)	1.918(1)
4	1.929(2)	1.945(3)	1.903(2)	2.004(3)	2.080(3)	1.975(3)
5	1.921(2)	1.890(2)	1.920(2)	1.942(2)	2.225(2)	1.997(2)
6	1.924(2)	1.904(3)	1.629(3)	2.311(3)	2.133(3)	1.946(3)

[a] Ref 5.

details of **6** will serve as a benchmark for the identification of the (L^{AP})$^-$ and (L^{AP}−H)$^{2-}$ oxidation level. The organic ligand is clearly bound in its trianionic form [(L^{AP})N(L^{AP}−H)]$^{3-}$. One amine group is deprotonated at N3 rendering it a coordinated amide; in addition, both phenol groups are deprotonated and

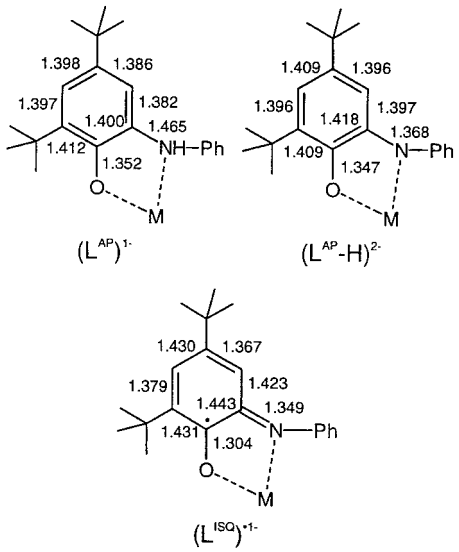

Figure 6. Average bond distances in (L^{AP})$^-$ and (L^{AP}−H)$^{2-}$, and (L^{ISQ})$^{\bullet -}$. The estimated error is ±0.015 Å. The sum of the six ring C−C bond distances in (L^{AP})$^-$ is 8.375 Å, in (L^{AP}−H)$^{2-}$ it is 8.425 Å, and in (L^{ISQ})$^{\bullet -}$ it is 8.473 Å.

coordinated to the vanadium ion. The nitrogen N3 is three-coordinate in a nearly planar geometry (sp^2 hybridization). In contrast, N1 and N2 are four-coordinate and sp^3-hybridized; the two amine protons have been located in the final difference Fourier map.

Since **6** contains a single V═O group where the terminal oxo ligand occupies the sixth coordination site, the central vanadium must be assigned an oxidation state +V (d^0). The V═O distance in **6** resembles closely vanadium(V) complexes containing a *cis*-dioxovanadium(V) moiety (V−O ∼ 1.65 Å).[10,11] The vanadium−amido V−N3 bond at 1.946(3) is the shortest V−N bond in **6,** and it is in *cis*-position relative to the V═O bond. The O3−V−N3 bond angle at 103.5(1)° is significantly larger than the ideal octahedral angle of 90°; the O3−V−N2 (amine) bond angle is normal at 89.9(1)°. In octahedral V(V) complexes with a *cis*-VO_2 unit the O−V−O bond angle is ∼107°.[11] Thus the *cis*-V(O3)(N3) unit in **6** is characteristic for a V(V) complex with a d^0 electron configuration.

The above analysis necessitates the oxidation level of the two di-*tert*-butyl ring systems of the ligand in **6** to be aromatic, i.e., an aminophenolate(1−) and an amidophenolate(2−) are present. These two moieties exhibit significant structural differences which are displayed schematically in Figure 6. The most striking difference is observed for the N−C aminophenyl bond lengths at 1.451(5) Å in the aminophenolate(1−) part and at 1.368(5) Å in the amidophenolate(2−) part. In contrast, the C−O distances at 1.349(5) and 1.347(5) Å are identical within experimental error; they are typical for phenolates.

It is an important feature of both the amino- and amidophenolato parts in **6** that the six aminophenol C−C bond distances are within experimental error of +0.015 Å (3σ) identical. The average C−C distance is 1.396 Å for the aminophenolato and 1.402 Å for the amidophenolato part. In the crystal structure of the uncoordinated ligand H[L^{AP}], the average C−C distance in the aminophenol part is 1.393 ± 0.015 Å.[4] The C−O bond length is 1.357, and the C−N distance of the aminophenol part

(10) Cornman, C. R.; Colpas, G. J.; Hoeschele, J. D.; Kampf, J.; Pecoraro, V. L. *J. Am. Chem. Soc.* **1992**, *114*, 9925.
(11) (a) Schulz, D.; Weyhermüller, T.; Wieghardt, K.; Nuber, B. *Inorg. Chim. Acta* **1995**, *240*, 217. (b) Neves, A.; Walz, W.; Wieghardt, K.; Nuber, B.; Weiss, J. *Inorg. Chem.* **1988**, *27*, 2484.

is 1.430 ± 0.015 Å. They are identical to those of the aminophenolato part in **6**. These results demonstrate that the ligand in **6** is an aromatic trianion, and the compound is correctly described with a physical oxidation state of +V for the vanadium ion.

We now describe the structures of the neutral octahedral complexes **1**−**3**, all of which contain three O,N-coordinated *o*-iminobenzosemiquinonato(1−) ligands, $(L^{ISQ})^{\bullet -}$. Complexes **1**, **2**, and also **4** crystallize in the orthorhombic chiral space group $P2_12_12_1$; only the cobalt complex **3** crystallizes in a different monoclinic space group $P2_1/n$. The neutral molecules in these compounds possess C_1 symmetry and exist in two enantiomeric forms. Thus, for **1**, **2**, and **4**, spontaneous enantiomeric resolution is observed, whereas the unit cell of **3** contains both enantiomers. We have not observed the C_3 symmetric diastereomer of any of the above compounds. Figure 3 shows a representative structure of these molecules.

As pointed out previously,[4,5] the three equidistant, short Co−O distances at 1.888 ± 0.003 Å together with three short Co−N distances at 1.934 ± 0.009 Å in **3** are only compatible with a low-spin d^6 configuration of a cobalt(III) ion. Similarly, the Cr−N and Cr−O distances in **1** summarized in Table 2 are typical for Cr(III), although it is noted that the three Cr−N and three Cr−O bond lengths are not equidistant within our small experimental error of only ±0.006 Å (3σ). Interestingly, the two Cr−O bonds in trans position relative to each other are the longest and nearly equidistant and, similarly, the two Cr−N bonds in trans position are significantly longer than the one in trans position to an oxygen donor.

As shown above, **2** contains a high-spin ferric ion and, consequently, the Fe−N and Fe−O bond lengths are the longest of the whole series of complexes; the Fe−O bond lengths are equidistant at 2.014 ± 0.009 Å, whereas the Fe−N distances are slightly different at 2.057, 2.149, and 2.091 Å. We cannot offer an explanation for this observation.

It is gratifying that the geometrical features of the three O,N-coordinate *o*-iminobenzosemiquinonato(1−) ligands are identical within our small experimental error limits, and, furthermore, these features do not vary appreciably with the nature of the central metal ion (Cr, Fe, Co). To calibrate our data we have summed up the six C−C bond distances for each individual aniline phenyl group in all complexes and determined the average C−C bond length to be 1.387 ± 0.015 Å. This part of the ligand is considered to be the most redox innocent one which is not affected by the actual oxidation level of the ligand or the nature of the coordinated metal ion. Within the small error limit all C−C distances of these phenyl rings are equidistant in all complexes—as expected.

In contrast, the iminobenzosemiquinonate part of these O,N-coordinated radicals exhibits significantly different C−C bond distances in the ring. Using the data of the tris(*o*-iminobenzosemiquinonato)metal complexes **1**−**3** compiled in Table S26 of the Supporting Information, we can derive the respective average bond distances for the ligand $(L^{ISQ})^{\bullet -}$ as shown in Figure 6. The average C−O and C−N bond lengths at 1.304 ± 0.015 and 1.349 ± 0.015 Å, respectively, are significantly shorter than the corresponding bond lengths in $(L^{AP})^-$ or $(L^{AP}-H)^{2-}$; they constitute the most significant structural parameters for the assignment of the oxidation level of a given ligand of this type in a coordination compound. Exactly the same parameters for the $(L^{ISQ})^{\bullet -}$ ligands have been found in the square-planar complexes $[M(L^{ISQ})_2]$ (M = Cu, Ni, Pd, Pt).[4]

Furthermore, the six ring C−C distances in the iminosemiquinonate part are not equidistant. We observe a typical pattern of a short (1.367 Å), a long (1.430 Å), and again a short (1.379 Å) C−C bond and three adjacent long C−C bonds. Thus this ring adopts a quinoid-type structure.

Table 3. Comparison of the Calculated and Observed Sums of the C−C Bond Lengths of the Aminophenol Rings in Octahedral Complexes **1**−**6**

no. of ligands			overall anionic charge[a]	calcd $\sum_1^{18}$ d(C−C),[b] Å	exptl $\sum_1^{18}$ d(C−C), Å (complex)
$(L^{ISQ})^{\bullet -}$	$(L^{AP}-H)^{2-}$	$(L^{AP})^-$			
3	0	0	3−	25.434	25.39 (**1**), 25.43 (**2**), 25.43 (**3**)
2	1	0	4−	25.366	
1	2	0	5−	25.298	25.27 (**4**)
0	3	0	6−	25.230	
0	2	1	5−	25.200	25.18 (**5**), 25.21 (**5**)
1	1	1	4−	25.245	

[a] Since the octahedral species $[ML_3]$ considered here are all neutral complexes, this number multiplied by −1 gives also the oxidation state of the respective metal ion. [b] The calculated values were obtained using average C−C bond distances in $(L^{ISQ})^{\bullet -}$, $(L^{AP})^-$, and $(L^{AP}-H)^{2-}$ given in Figure 6. The sum of the respective number of $(L^{ISQ})^{\bullet -}$, $(L^{AP}-H)^{2-}$, and $(L^{AP})^-$ ligands is always 3.

In the following we also use a parameter which is obtained from the sum of the six C−C bond distances in the aminophenol derived part of the ligand. For $(L^{AP})^-$ this sum is 8.375 ± 0.03 Å, for $(L^{AP}-H)^{2-}$ it is 8.425 ± 0.03 Å, and for $(L^{ISQ})^{\bullet -}$ it is 8.473 ± 0.03 Å. It is noted that this parameter for the *phenyl* ring part of all three ligand types is constant at 8.322 ± 0.03 Å. Thus the attachment of an amino (or amido) and a phenolate oxygen in the ortho-position (plus two *tert*-butyl groups) in aromatic $(L^{AP})^-$ and $(L^{AP}-H)^{2-}$ enforces a slight—but significant—expansion of the aromatic ring. The difference between $(L^{AP})^-$ and $(L^{AP}-H)^{2-}$ is at the limit of significance, but the latter appears to be slightly more expanded than the former. Significantly, this sum is the largest for the iminosemiquinonate radicals, $(L^{ISQ})^{\bullet -}$.

The most difficult cases for the assignment of oxidation states (levels) of the ligands and the central metal ion are the vanadium complexes **4** and **5**. Complex **4** crystallizes in the same chiral space group $P2_12_12_1$ as **1** and **3**. Should we therefore describe **4** as $[V^{III}(L^{ISQ})_3]$, or $[V^{IV}(L^{AP}-H)(L^{ISQ})_2]$, or even $[V^{V}(L^{ISQ})(L^{AP}-H)_2]$?

Inspection of the data in Table S26 suggests that this species contains two ligands with identical oxidation level and a third, different one. The latter displays the shortest C−O and C−N distances of the three, and the six C−C distances in the ring display the typical short−long−short pattern of a coordinated $(L^{ISQ})^{\bullet -}$. On the other hand, the other two rings closely, but not fully, meet the requirements for coordinated $(L^{AP}-H)^{2-}$. Inspection of the thermal parameters of the ring C atoms in **4** reveals that they are on average 10−20% larger than those in all other structures. This may reflect a static or dynamic disorder in the structure of **4**. This effect is small and just outside our level of significance.

Therefore, we have calculated the expected sum of the aminophenol ring C−C distances over all three ligands in **4,** which is 25.283 Å. By using the data in Figure 6, we can calculate the same sum for three $(L^{ISQ})^{\bullet -}$ ligands to be 25.419 Å, or for a combination of two $(L^{ISQ})^{\bullet -}$ and one $(L^{AP}-H)^{2-}$ it is 25.371 Å, or, alternatively, for a combination of one $(L^{ISQ})^{\bullet -}$ and two $(L^{AP}-H)^{2-}$ it is 25.323 Å (Table 3). Clearly, good agreement is observed for a ligand distribution $[V^{V}(L^{ISQ})(L^{AP}-H)_2]$ for **4**. We stress again that our significance level does not have—per se—the resolution necessary to unambiguously support this conclusion.

Table 4. Redox Potentials of Complexes from Cyclic Voltammetry[a] and Coulometry

		redox potentials, V vs Fc^+/Fc couple					
complex	1[b]	2	3	4	5	6[c]	*T*, °C
1 Cr	1.10	0.64	−0.10	−1.26	−1.77		20
2 Fe		0.27	−0.35	−1.12	−1.31	−1.51*	−40
3 Co		0.20	−0.34	−0.99	−1.31		20
4 V		−0.10	−0.89	−1.66	−2.13		−2

[a] Conditions: CH_2Cl_2 solution containing 0.10 M [TBA]PF_6 supporting electrolyte; glassy carbon working electrode; ferrocene internal standard; ~1 mM [complex]. [b] 1, $[M(L^{IBQ})_2(L^{ISQ})]^{2+}/[M(L^{IBQ})(L^{ISQ})_2]^+$; 2, $[M(L^{IBQ})(L^{ISQ})_2]^+/[M(L^{ISQ})_3]^0$; 3, $[M(L^{ISQ})_3]^0/[(L^{AP}-H)(L^{ISQ})_2]^-$; 4, $[M(L^{AP}-H)(L^{ISQ})_2]^-/[M(L^{AP}-H)_2(L^{ISQ})]^{2-}$; 5, $[M(L^{AP}-H)_2(L^{ISQ})]^{2-}/[M(L^{AP}-H)_3]^{2-}$; 6, $[M^n(L^{AP}-H)_3]/[M^{n-1}(L^{AP}-H)_3]^{4-}$ for complexes **1**−**3**. [c] Value marked with an asterisk is from an irreversible process; $E_{p,red}$ is given.

The problem for complex **5** is less difficult, because the presence of an $(L^{AP})^-$ ligand is readily detected in the structure by its sp^3-hydrized nitrogen donor which carries a proton. In principle, we have to discern between the following charge distributions: $[V^{III}(L^{AP})(L^{ISQ})_2]$, $[V^{IV}(L^{AP})(L^{AP}-H)(L^{ISQ})]$, and $[V^{V}(L^{AP})(L^{AP}-H)_2]$. The situation is complicated by the fact that there are two crystallographically independent neutral molecules in the unit cell, but these two are within experimental error identical with the exception that the phenyl rings of one of the coordinated $(L^{AP}-H)^{2-}$ ligands possess two different orientations relative to the amidophenolato ring; this is shown in Figure S4 of the Supporting Information. The dimensions of the protonated ligands $(L^{AP})^-$ in **5** are identical to those given in Figure 6. Thus, we have to consider the following charge distributions for the remaining two ligands in molecule of **5**: two $(L^{ISQ})^{\bullet-}$ vs two $(L^{AP}-H)^{2-}$ or a statistical distribution of one $(L^{AP}-H)$ and one $(L^{ISQ})^{\bullet-}$. If we calculate the sum of the ring C−C distances using data from Figure 6 for these three possibilities, we obtain 16.946, 16.850, and 16.898 Å, respectively. Experimentally, we find 16.804 and 16.825 Å for the two independent molecules in **5,** which indicates a charge distribution as in $[V^{V}(L^{AP})(L^{AP-}H)_2]$. The observed average C−O and C−N distances for $(L^{AP})^-$ in the two molecules are in excellent agreement with this assignment. The same is true for the average C−O and C−N distances for both $(L^{AP}-H)^{2-}$ ligands in both molecules at 1.330, 1.335 Å and 1.385, 1.387 Å, respectively.

Spectro- and Electrochemistry. Cyclic and, in some cases, square-wave voltammograms have been recorded in CH_2Cl_2 solutions of complexes containing 0.10 M [TBA]PF_6 as supporting electrolyte at a glassy carbon working electrode and a $Ag/AgNO_3$ reference electrode. Ferrocene was used as an internal standard, and potentials are referenced versus the ferrocenium/ferrocene couple (Fc^+/Fc). Table 4 summarizes these results; the electronic spectra of complexes **1**−**6** are given in Table 5.

Figure 7 shows the cyclic voltammograms (cvs) of **1** and **3**. We present these data first because Cr^{III} and low-spin Co^{III} ions are expected to be redox-inert and all observed redox activity can, therefore, be ascribed to ligand-based processes. The cv of **1** displays five reversible one-electron-transfer waves in the range +1.5 to −2.0 V. From coulometric measurements at appropriately fixed potentials it was established that three waves at 1.10, 0.64, and −0.10 V correspond to one-electron oxidations of $[Cr^{III}(L^{ISQ})_3]$ and the waves at −1.26 and −1.77 V correspond to two successive one-electron reductions of **1**. Thus, the sequences shown in eqs 1 and 2 summarize the electrochemical behavior, where $(L^{IBQ})^0$ represents the *o*-iminobenzoquinone oxidation level.

Table 5. Electronic Spectra of Complexes in CH_2Cl_2 Solutions

complex	λ, nm (ϵ, L mol^{-1} cm^{-1})
1	239 (4.5×10^4), 297 (1.9×10^4), 526 (1.7×10^4), 746 (4.1×10^3)
2	231 (4.4×10^4), 306 (2.0×10^4), 423 (6.0×10^3), 746 (8.4×10^3)
3	233 (5.2×10^4), 283 (2.3×10^4), 675 (1.3×10^4), 901 (1.6×10^4)
4	238 (3.7×10^4), 279 (2.2×10^4), 598 (2.3×10^4), 929 (7.1×10^3)
6[a]	353 (5.1×10^3), 470 sh, 530 (5.5×10^3), 1047 (5.2×10^3)

[a] Measured in THF.

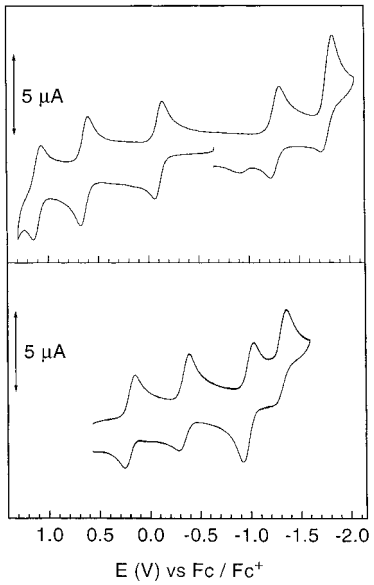

Figure 7. Cyclic voltammograms of **1** (top) and **3** (bottom) in CH_2Cl_2 (0.10 M [TBA]PF_6) at 20 °C and a scan rate of 200 mV s^{-1}.

$$[Cr^{III}(L^{IBQ})_3]^{3+} \underset{-e}{\overset{+e}{\rightleftharpoons}} [Cr^{III}(L^{ISQ})(L^{IBQ})_2]^{2+} \underset{-e}{\overset{+e}{\rightleftharpoons}} [Cr^{III}(L^{ISQ})_2(L^{IBQ})] \underset{-e}{\overset{+e}{\rightleftharpoons}} \mathbf{1} \quad (1)$$

$$\mathbf{1} \underset{-e}{\overset{+e}{\rightleftharpoons}} [Cr^{III}(L^{ISQ})_2(L^{AP}-H)]^- \underset{-e}{\overset{+e}{\rightleftharpoons}} [Cr^{III}(L^{ISQ})(L^{AP}-H)]^{2-} \quad (2)$$

The fully reduced $[Cr^{III}(L^{AP}-H)]^{3-}$ form is not accessible even at −2.0 V.

Similarly, the cv of **3** displays two reversible one-electron oxidation waves and two successive one-electron reduction waves which we assign as

$$[Co^{III}(L^{ISQ})(L^{IBQ})_2]^{2+} \underset{-e}{\overset{+e}{\rightleftharpoons}} [Co^{III}(L^{ISQ})_2(L^{IBQ})]^{+} \underset{-e}{\overset{+e}{\rightleftharpoons}} [Co^{III}(L^{ISQ})_3] \quad (3)$$

$$[Co^{III}(L^{ISQ})_3] \underset{-e}{\overset{+e}{\rightleftharpoons}} [Co^{III}(L^{AP}-H)(L^{ISQ})_2]^- \underset{-e}{\overset{+e}{\rightleftharpoons}} [Co^{III}(L^{AP}-H)_2(L^{ISQ})]^{2-} \quad (4)$$

In this instance both the fully oxidized form $[Co^{III}(L^{IBQ})_3]^{3+}$ and the fully reduced form $[Co^{III}(L^{AP}-H)_3]^{3-}$ are electrochemically not accessible. We note that it is more difficult to oxidize **1** than **3** by 400 mV for the second oxidation step and by 220 mV for the first. Chromium(III) is a stronger Lewis acid than

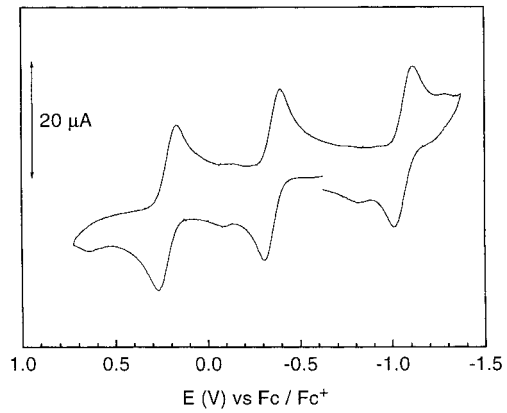

Figure 8. Cyclic voltammograms of **2** at −40 °C in CH_2Cl_2 solution (0.10 M [TBA]PF_6) and a scan rate of 400 mV s^{-1}.

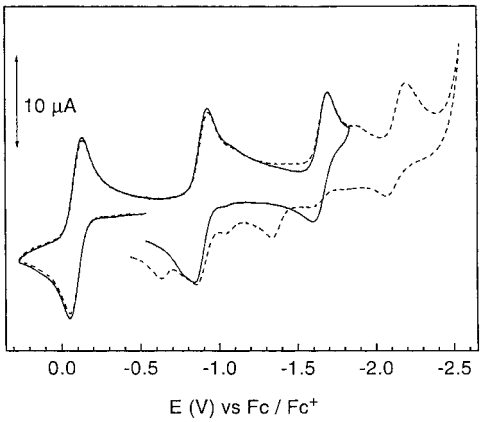

Figure 9. Cyclic voltammograms of **4** in CH_2Cl_2 solution (0.20 M [TBA]PF_6) at a scan rate of 200 mV s^{-1} at −20 °C.

cobalt(III). In contrast, it is more difficult to reduce **3** than **1** by ∼400 mV because the ligands in **4** are electron richer than those in **1** for the same reason.

The cv of the ferric complex **2** shown in Figure 8 has been recorded at −40 °C and fast scan rates because the reduced and oxidized forms are quite labile. The cv is essentially identical to that of **3**—even the redox potentials are rather similar. A fifth irreversible wave at −1.51 V (not shown) may involve a metal-centered reduction generating $[Fe^{II}(L^{AP}-H)_3]^{4-}$.

While the cvs of **1**−**3** are quite similar and apparently involve the same ligand-centered processes at similar potentials, the cv of **4** is distinctly different. Figure 9 shows its cyclic voltammogram. Four reversible, one-electron-transfer waves are observed at −0.10, −0.89, −1.66, and −2.13 V. The first corresponds to a one-electron oxidation of **4,** whereas the latter three are one-electron reductions. The observation that the two peaks at −1.66 and −2.13 V display a reduced peak current (by ∼35%) compared to the peaks at −0.10 and −0.89 V probably relates to protonation effects of the highly negatively charged anions by trace amounts of water in our solvent CH_2Cl_2. These protonated forms may then be reoxidized at ∼−0.9 and −1.7 V as evidenced by very small peaks in the square-wave voltammograms (swv) at these potentials. We did not investigate this effect in more detail.

Since the starting material **4** contains $[V^{V}(L^{AP}-H)_2(L^{ISQ})]$ molecules, the one-electron oxidation must correspond to the generation of a monocation $[V^{V}(L^{AP}-H)(L^{ISQ})_2]^{+}$, whereas the first reduction produces a diamagnetic monoanion of unknown charge distribution. $[V^{V}(L^{AP}-H)_3]^{-}$ or $[V^{IV}(L^{AP}-H)_2(L^{ISQ})]^{-}$ must be considered—even $[V^{III}(L^{AP}-H)(L^{ISQ})_2]^{-}$ is a possibility. Similarly, for the dianions and trianions produced after the second and third reductions, respectively, species with differing charge distributions must be considered.

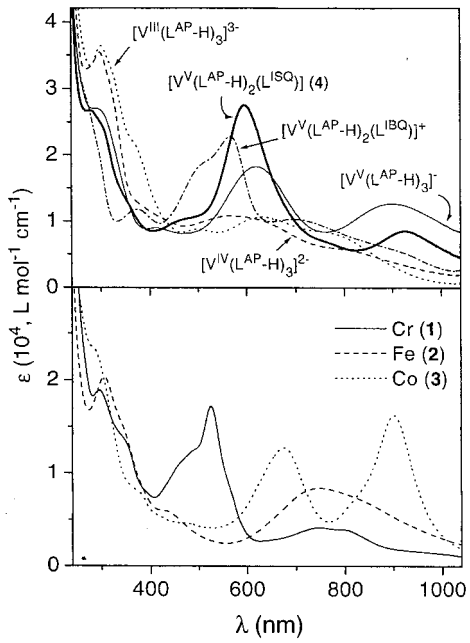

Figure 10. Electronic spectra of **4** and its electrochemically generated monocation, mono-, di-, and trianion in CH_2Cl_2 solution (0.10 M [TBA]-PF_6) at −20 °C (top). Bottom: Electronic spectra of **1**−**3** in CH_2Cl_2 at 20 °C.

To obtain more information, we have recorded the electronic spectra of the electrochemically oxidized and reduced species by using an OTTLE cell. Figure 10 (top) exhibits these spectra. Interestingly, the starting material **4**, its monoanion and -cation display very intense, $\epsilon > 1.8 \times 10^4$ M^{-1} cm^{-1}, charge-transfer (CT) absorption maxima in the visible in the range 500−700 nm. These bands are not observed in $[LCu^{II}(L^{AP}-H)]^{0}$, $[LCu^{II}(L^{ISQ})]^{+}$, or $[LCu^{II}(L^{IBQ})]^{2+}$ and, therefore, cannot be assigned to intraligand CT processes.[4] These transitions are typical for ligand-to-V^{V} CT bands (LMCT). We conclude that these spectra imply the following charge distributions: $[V^{V}(L^{AP}-H)_2(L^{ISQ})]$ in the neutral species **4**—in excellent agreement with its structure and EPR spectrum (see above)—$[V^{V}(L^{AP}-H)(L^{ISQ})_2]^{+}$, and $[V^{V}(L^{AP}-H)_3]^{-}$. The dianion must then contain a vanadium(IV) center; i.e., the reduction of the monoanion is metal-centered producing $[V^{IV}(L^{AP}-H)_3]^{2-}$.

To explore the correctness of this assignment, we have recorded the X-band EPR spectrum of the electrochemically generated dianion. This spectrum and its simulation are shown in Figure 2 (bottom). The X-band EPR spectrum recorded on a frozen solution of CH_2Cl_2 of doubly reduced **4** (∼1.0 mM) clearly reveals the V(IV) character of this dianion. A typical, well-resolved ^{51}V(IV) ($S = {}^1/_2$, $I = {}^7/_2$) hyperfine pattern is observed. The spectrum was simulated by using principal g values $g_1 = 1.984$, $g_2 = 1.963$, $g_3 = 1.967$ and ^{51}V hyperfine tensor components $A_1 = 6.8 \times 10^{-4}$ cm^{-1}, $A_2 = 47.4 \times 10^{-4}$ cm^{-1}, $A_3 = 121.2 \times 10^{-4}$ cm^{-1}. Particularly the isotropic part, $A_{iso} = (1/3)\mathrm{Tr}(\mathbf{A}) = 64 \times 10^{-4}$ cm^{-1}, is a perfect match with the values reported for other vanadium(IV) complexes,[12] $A_{iso} = (59-80) \times 10^{-4}$ cm^{-1}, including an example of a tris-

(12) (a) Atherton, N. M.; Winscom, C. J. *Inorg. Chem.* **1973**, *12*, 383. (b) Diamantis, A. A.; Raynor, J. B.; Rieger, P. H. *J. Chem. Soc., Dalton Trans.* **1980**, 1980. (c) Jezierski, A.; Raynor, J. B. *J. Chem. Soc., Dalton Trans.* **1981**, 1−7.

catecholate compound[13] ($A_{iso} = 76 \times 10^{-4}$ cm^{-1}). We note that these values are somewhat lower than those of vanadyl complexes ($A_{iso} = (80-100) \times 10^{-4}$ cm^{-1}). Hence, the $S = {}^1/_2$ ground state of the dianion owes its origin basically to a $3d^1$ electron configuration of V(IV).

The nature of the orbital ground state is less clear than the metal character of the magnetic orbital. The **g** and the **A** tensors are both rhombic, and the values are neither close to the limit ($g_i < g_x,g_y < 2$, $A_z \gg A_x,A_y$) nor to ($g_z \approx 2$, $g_x,g_y < 2$; $A_z \ll A_x,A_y$). The first case would be characteristic of a d_{xy} ground state in octahedral symmetry, whereas the second is expected for a d_z^2 state which typically arises from trigonal symmetry.[12,13] Since all *g* values are significantly smaller than 2.002 and there is only one large *A* value (in the direction of a small *g* value), we discard the d_z^2 state. The ground state is best described as a d_{xy} state with considerable orbital mixture due to a basically octahedral symmetry with tetragonal and/or trigonal distortion. The last reductive step must then generate [$V^{III}(L^{AP}-H)_3$]$^{3-}$.

Discussion

Having established the charge distribution in complexes **1**−**6** in a consistent manner by high-quality single-crystal X-ray crystallography and spectroscopy as well as magneto- and electrochemistry, we now discuss in detail similarities and differences of octahedral catecholato(2−) (Cat.), *o*-semiquinonato(1−) (SQ), and benzoquinonate (BQ) complexes of V, Cr, Fe, and Co with those containing amino-, amidophenolato, and *o*-iminobenzosemiquinonato ligands studied here.

In a series of seminal papers Pierpont, Raymond, Gatteschi, Hendrickson, and co-workers have reported on the amazing variety of electronic structures of complexes containing unsubstituted catecholates (and their oxidized derivatives), tetrachlorocatecholates, and, most pertinent for our purposes, 3,5-di-*tert*-butylcatecholates and 3,6-di-*tert*-butylcatecholates and of their respective oxidized forms.[1,2] We will focus on the coordination chemistry of the latter two ligands, (3,5-Cat.) and (3,6-Cat.), since they resemble most closely the present ligands ($L^{AP}-H)^{2-}$, (L^{AP})$^-$, and (L^{ISQ})$^{\bullet-}$.

The [Cr^{III}(3,5-SQ)$_3$] complex[14] is diamagnetic and undergoes in solution three successive ligand-based one-electron oxidations yielding the trication [$Cr^{III}(BQ)_3$]$^{3+}$ ($S = {}^3/_2$) and, similarly, three successive ligand-based one-electron reductions yielding [Cr^{III}(Cat.)$_3$]$^{3-}$ ($S = {}^3/_2$). The chemistry and electronic structures of the analogous series of complexes derived from **1** (eqs 1 and 2) is very similar with the exception that the [$Cr^{III}(L^{AP}-H)_3$]$^{3-}$ species is electrochemically not accessible. The electronic structure and EPR properties of the individual members of the series have been elegantly described in ref 15. A completely analogous description is valid for **1** and its oxidized or reduced derivatives. The ground state of these species is attained via very strong antiferromagnetic coupling between the half-filled t_{2g}^3 subshell of the Cr^{III} ion and one, two, or three ligand radicals. Excited states are not populated at room temperature.

The electronic spectrum of **1** displays the same unusual features as [$Cr^{III}(SQ)_3$] species.[14b,c] In agreement with Dei et al.,[16] we assign the intense peak of **1** at ∼550 nm to a spin-forbidden transition $^4A_{2g} \rightarrow {}^2E_g$ corresponding to a spin flip in the ground state. This transition gains intensity by 3 orders of magnitude by the strong antiferromagnetic exchange coupling between the Cr^{III} ion and the three (L^{ISQ})$^{\bullet-}$ radicals. This transition has also been observed in tris(phenoxyl)chromium(III) complexes.[17]

[$Co^{III}(SQ)_3$] complexes are rare, but the structure of [Co^{III}(3,6-SQ)$_3$] has been reported.[18] It possesses an $S = {}^1/_2$ ground state and displays an EPR spectrum at 77 K typical for a ligand radical with a ^{59}Co hyperfine coupling of 22.6 G. In contrast, **3** has an $S = {}^3/_2$ ground state. Thus, in [Co^{III}(3,6-SQ)$_3$] the SQ−SQ coupling is antiferromagnetic, whereas in **3** it is ferromagnetic. This behavior has been interpreted in ref 4. [Co(3,6-SQ)$_3$] is not stable in solution, and, therefore, its electrochemistry has not been studied, in contrast to **3**. For **3**, neither the fully oxidized form [$Co^{III}(L^{IBQ})$]$^{3+}$ nor the fully reduced form [Co^{III}-($L^{AP}-H)_3$]$^{3-}$ are electrochemically accessible in the usual potential range 0.5 to −2.0 V vs Fc^+/Fc.

[$Fe^{III}(SQ)_3$] complexes are spectroscopically and structurally well-characterized.[14b,19−23] All of them possess an $S = 1$ ground state which is again attained via strong antiferromagnetic coupling between the half-filled t_{2g} level of the ferric metal ion and three semiquinonate radicals. Excited states ($S = 2-4$) are populated at room temperature, giving rise to a temperature dependence of the effective moment.[14b] Mössbauer spectroscopy has unequivocally shown that a d^5 configurated ferric ion is present.[14b] Complex **2** resembles in all aspects these features. It is only remarkable that the electrochemistry of **2** has allowed the generation of [$Fe^{II}(L^{AP}-H)_3$]$^{4-}$ at −1.51 V. [Fe^{II}(Cat.)$_3$]$^{4-}$ species have not been reported, but (trisphenolato)iron(II) complexes have been described; their redox potential for the [Fe^{III}(phenolato)$_3$]^0/[Fe^{II}(phenolato)$_3$]$^-$ couple has been reported at −1.7 V vs Fc^+/Fc.[9]

The coordination chemistry of vanadium with noninnocent ligands is rather complicated and the actual charge distribution in such species is often quite controversial.[24,25] For example, there are two neutral vanadium complexes containing three catecholate derived bidentate ligands reported, which are described as [$V^{III}(SQ)_3$] species. The structures of [V(3,5-SQ)$_3$][24b] and [V(Cl_4SQ)$_3$][24a] have not been established by X-ray crystallography due to problems encountered by their oxygen sensitivity and loss of solvent molecules of crystallization. A third species of this type [V(phenSQ)$_3$] (the ligand phenSQ$^{\bullet-}$ is derived from 9,10-phenanthrenequinone by 1e reduction) has also been described.[25] Its structure has also not been reported, but an assignment as tris(semiquinonato)vanadium(III) has been suggested.

(13) Branca, M.; Micera, G.; Dessi, A.; Sanna, D.; Raymond, K. N. *Inorg. Chem.* **1990**, *29*, 1586.
(14) (a) Pierpont, C. G.; Downs, H. H. *J. Am. Chem. Soc.* **1976**, *98*, 4834. (b) Buchanan, R. M.; Kessel, S. L.; Downs, H. H.; Pierpont, C. G.; Hendrickson, D. N. *J. Am. Chem. Soc.* **1978**, *100*, 7894. (c) Sofen, S. R.; Ware, D. C.; Cooper, S. R.; Raymond, K. N. *Inorg. Chem.* **1979**, *18*, 234. (d) Downs, H. H.; Buchanan, R. M.; Pierpont, C. G. *Inorg. Chem.* **1979**, *18*, 1736.
(15) Dei, A.; Gatteschi, D. *Inorg. Chim. Acta* **1992**, *198*−*200*, 813.
(16) Benelli, C.; Dei, A.; Gatteschi, D.; Güdel, H. U.; Pardi, L. *Inorg. Chem.* **1989**, *28*, 3089.
(17) Sokolowski, A.; Bothe, E.; Bill, E.; Weyhermüller, T.; Wieghardt, K. *Chem. Commun.* **1996**, 1671.
(18) Lange, C. W.; Conklin, B. J.; Pierpont, C. G. *Inorg. Chem.* **1994**, *33*, 1276.
(19) Attia, A. S.; Conklin, B. J.; Lange, C. W.; Pierpont, C. G. *Inorg. Chem.* **1996**, *35*, 1033.
(20) Buchanan, R. M.; Downs, H. H.; Shorthill, W. B.; Pierpont, C. G.; Hendrickson, D. N. *J. Am. Chem. Soc.* **1978**, *100*, 4318.
(21) Lynch, M. W.; Valentine, M.; Hendrickson, D. N. *J. Am. Chem. Soc.* **1982**, *104*, 6982.
(22) Funabiki, T.; Mizoguchi, A.; Sugimoto, T.; Tada, S.; Tsuji, M.; Sakamoto, H.; Yoshida, S. *J. Am. Chem. Soc.* **1986**, *108*, 2921.
(23) Boone, S. R.; Purser, G. H.; Chang, H.-R.; Lowery, M. D.; Hendrickson, D. N.; Pierpont, C. G. *J. Am. Chem. Soc.* **1982**, *111*, 2292.
(24) (a) Cass, M. E.; Gordon, N. R.; Pierpont, C. G. *Inorg. Chem.* **1986**, *25*, 3962. (b) Cass, M. E.; Greene, D. L.; Buchanan, R. M.; Pierpont, C. G. *J. Am. Chem. Soc.* **1983**, *105*, 2680. (c) Cooper, S. R.; Koh, Y. G.; Raymond, K. N. *J. Am. Chem. Soc.* **1982**, *104*, 5092.
(25) Calderazzo, F.; Pampaloni, G. *J. Organomet. Chem.* **1987**, *330*, 47.

Scheme 2. Comparison of Species Accessible from **4** and $[V(SQ)_3]$ (or $[V^V(Cat.)_2(SQ)]$)

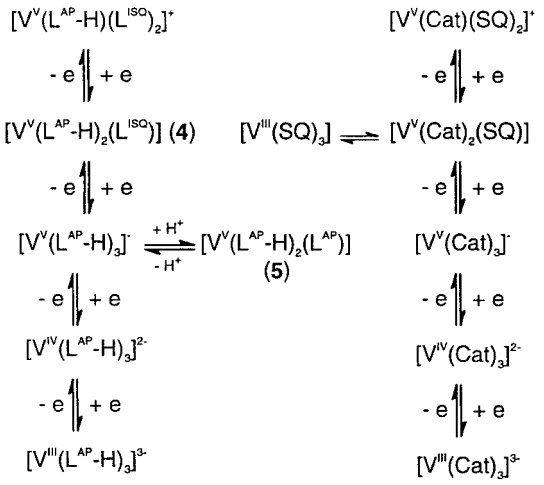

The charge distribution as $[V^{III}(SQ)_3]$ has been inferred from the observation that the corresponding $[Cr^{III}(SQ)_3]$, $[Fe^{III}(SQ)_3]$ complexes are isomorphous; i.e., the three complexes crystallize in the same space group.[24] Also, the similarity of the IR spectra of these species has been put forward as evidence for the $[V^{III}(SQ)_3]$ formulation. On the other hand, solution EPR spectra conclusively show that these species with an $S = {}^1/_2$ ground state have the unpaired electron predominantly localized on one semiquinonato ligand[23] which requires a charge distribution close to $[V^V(Cat.)_2(SQ)]$.[13] This distribution is felt to be more in agreement with the observed electrochemistry (see below).

Pierpont et al.,[24a,b] on the other hand, interpret the electronic structure of $[V^{III}(SQ)_3]$ complexes in the solid state as arising from "strong antiferromagnetic coupling between paramagnetic radical ligands and the d^2 metal ion". They consider a distribution $[V^V(Cat.)_2(SQ)]$ for the neutral species in solution. Thus for the neutral complex $[V^{III}(Cl_4SQ)_3]$ two interconvertible redox isomers have been proposed to exist.

The electronic structure of **4** in the solid state *and* in solution is clearly $[V^V(L^{AP}-H)_2(L^{ISQ})]$. Since **1**, **2**, and **4** crystallize in the same space group, the assignment of $[V^{III}(SQ)_3]$ based on the above crystallographic argument must be discarded. It is also noted that the IR spectra of all complexes reported here are similar and do not allow one to distinguish the differing oxidation levels of the ligands.

In Scheme 2 we compare the redox chemistry of **4** with that reported for $[V^{III}(Cl_4SQ)_3]$.[24] Both species exist in five oxidation levels which differ successively by one electron. We have assigned the electronic structures of the mono-, di-, and trianions of **5** as $[V^V(L^{AP}-H)_3]^-$, $[V^{IV}(L^{AP}-H)_3]^{2-}$, and $[V^{III}(L^{AP}-H)_3]^{3-}$; i.e., the two reduction steps mono- to di-, and di- to trianion are metal-centered. Once the V^V level is reached at the $[V^V(L^{AP}-H)_3]^-$ level, two one-electron oxidations are observed which are ligand-based. Thus, **4** and the monocation $[V^V(L^{AP}-H)(L^{ISQ})_2]^+$ are generated. The $[V^V(L^{ISQ})_3]^{2+}$ level is electrochemically not accessible in the potential range employed.

Exactly the same scheme applies for $[V^V(Cat.)_2(SQ)]^0$, where the mono-,[24] di-,[26] and trianionic[27] forms have been isolated as salts and their structures have been determined by X-ray crystallography. They unambiguously correspond to the series $[V(Cat.)_3]^{-,2-,3-}$ involving V^V d^0, V^{IV} d^1, and V^{III} d^2, respectively. The EPR spectrum of $[V^{IV}(Cat.)_3]^{2-}$ has been reported;[28] it is similar to that reported here for $[V^{IV}(L^{AP}-H)_3]^{2-}$ with the exception that **4** has a d_{xy} ground state, whereas the $[V^{IV}(Cat.)_3]^{2-}$ species has a d_z^2 ground state. The monoanion of **4** can be reversibly protonated and the neutral complex **5** has been isolated. Its crystal structure unambiguously demonstrates a charge distribution $[V^V(L^{AP}-H)_2(L^{AP})]$.

Acknowledgment. H.C. thanks the Alexander von Humboldt Foundation for a fellowship, and C.N.V. is grateful for a Max-Planck stipend. We thank the Fonds der Chemischen Industrie for financial support.

Supporting Information Available: Figures showing the Mössbauer spectrum of **2**, the structures of **1** and **4**, and an overlay of the two molecules in crystals of **4**, respectively, and tables summarizing crystal data, atomic coordinates, bond lengths and angles, displacement parameters, and hydrogen coordinates of complexes **1**−**6**. Five X-ray crystallographic files, in CIF format. This material is available free of charge via the Internet at http://pubs.acs.org.

IC010106A

(26) Cooper, S. R.; Koh, Y. B.; Raymond, K. N. *J. Am. Chem. Soc.* **1982**, *104*, 5092.
(27) Bulls, A. R.; Pippin, C. G.; Halm, F. E.; Raymond, K. N. *J. Am. Chem. Soc.* **1990**, *112*, 2627.
(28) Branca, M.; Micera, G.; Dessi, A.; Sanna, D.; Raymond, K. N. *Inorg. Chem.* **1990**, *29*, 1586.